# Development of a rapid and sensitive CasRx-based diagnostic assay for SARS-CoV-2

Daniel J Brogan[1,¶], Duverney Chaverra-Rodriguez[1¶], Calvin P Lin[2,¶], Andrea L Smidler[1,&], Ting Yang[1,&], Lenissa M. Alcantara[1], Igor Antoshechkin[3], Junru Liu[1], Robyn R Raban[1], Pedro Belda-Ferre[4], Rob Knight[4-7], Elizabeth A Komives[2], Omar S. Akbari[1,*]

[1]Division of Biological Sciences, Section of Cell and Developmental Biology, University of California, San Diego, La Jolla, CA, 92093.

[2]Department of Chemistry and Biochemistry, University of California, San Diego, La Jolla, CA 92092.

[3]Division of Biology and Biological Engineering, California Institute of Technology, Pasadena, CA 91125

[4]Department of Pediatrics, University of California San Diego, La Jolla, CA 92161

[5]Center for Microbiome Innovation, University of California San Diego, La Jolla, CA 92093

[6]Department of Computer Science and Engineering, University of California San Diego, La Jolla, CA 92093

[7]Department of Bioengineering, University of California San Diego, La Jolla, CA 92093

[*]Correspondence to: Omar S. Akbari, (oakbari@ucsd.edu)

[¶]equal first author contributions
[&]equal second author contributions

## SUPPLEMENTARY FIGURES

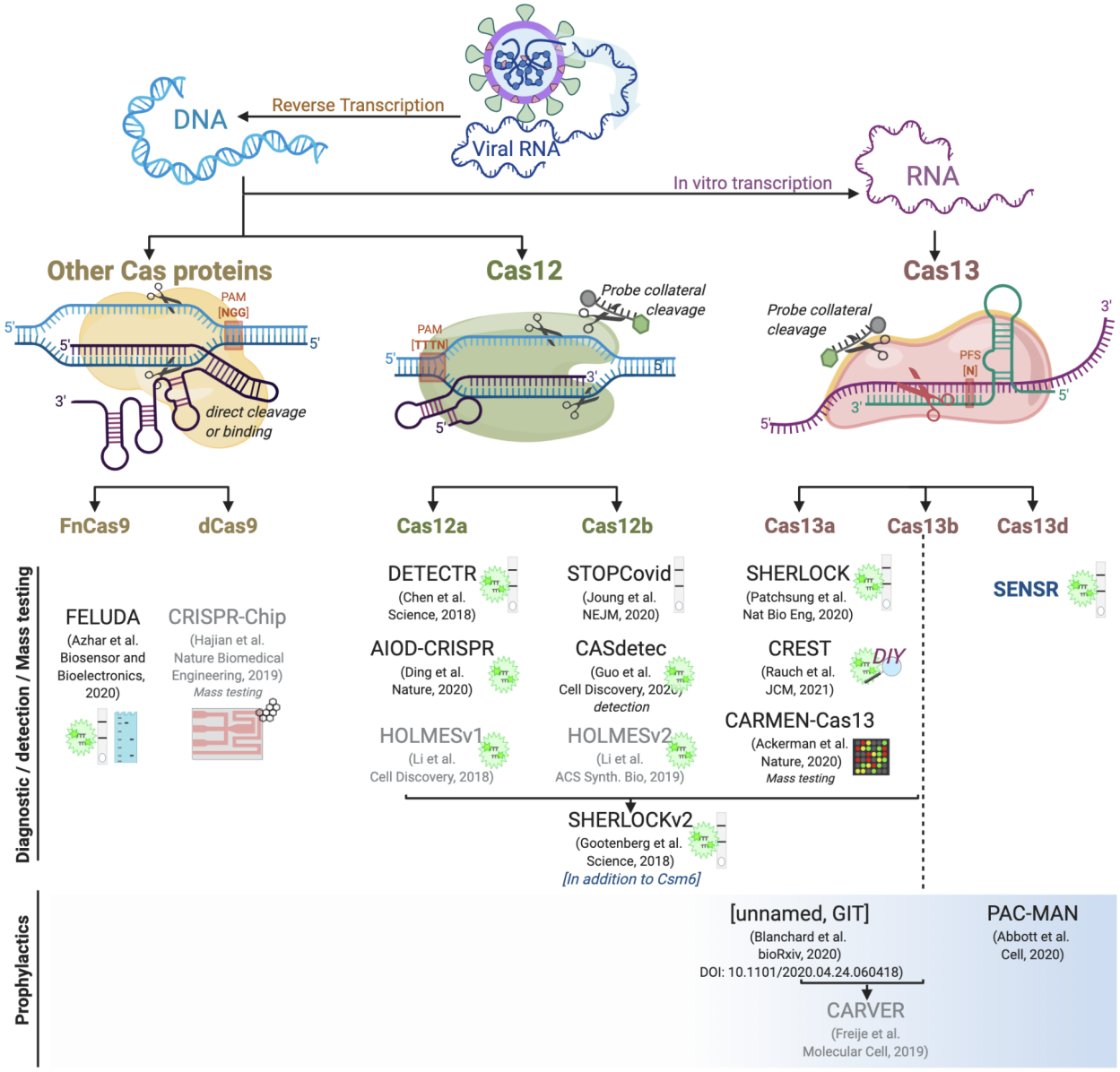


**Supplementary Figure 1. Summary of current CRISPR-based anti-Covid technologies organized by Cas enzyme used and by role as diagnostic or detection tool, or as a putative prophylactic.** Those technologies shown in black font have been demonstrated to have explicit activity against SARS-CoV-2, while those technologies shown in grey font have been publicly discussed or proposed to be technological candidates for SARS-CoV-2 detection or prophylaxis, however have not yet been fully demonstrated/optimized for said purpose as of the publication of this manuscript. Some technologies have not yet been given a formal name by their authors, and are therefore denoted as 'unnamed' followed by the acronym for the primary institutional affiliation behind the work. To better identify and distinguish these technologies, the DOI has been provided. **[Diagnostics/detection systems/Mass testing]** For all technologies viral RNA is extracted, reverse transcribed into cDNA, followed by template amplification by either PCR, RPA or LAMP, then input into subsequent

reactions with the exception of CRISPR-Chip which does not require an amplification step. Cas12-based enzymes, as well as many other Cas proteins (including Cas9) recognize DNA species, while Cas13-based enzymes recognize ssRNA, and all can be used to detect evidence of specific sequences by fluorescence or lateral flow. The detection method for each technology is noted with the presence of an icon adjacent. The majority of the technologies summarized here use fluorescence or lateral flow or both. The lime glow icon indicates readout by fluorescence, while the grey bar indicates read-out by lateral flow. Some of the other technologies can be read out by different detection methods. Notably because FELUDA relies on direct sequence cleavage, and not the collateral cleavage property shared amongst the Cas12- and Cas13-based technologies, it can also be analyzed by gel electrophoresis as evidence of distinct band cleavage (aqua gel icon). Also, CRISPR-Chip has been discussed as a SARS-CoV-2 mass detection candidate, though these findings have not yet been made publicly available. Read-out by this technology is achieved via a graphene-based transistor (icon is red, grey with graphene structure adjacent). Other different technologies include CREST, which achieves detection via fluorescence using a distinctly do-it-yourself (DIY) BioHacking approach, by utilizing equipment easily procured and operated by novice scientists, as well as CARMEN-Cas13 which detects evidence of SARS-CoV-2 sequences by microarray. The technology outlined here is an addition to current SHERLOCK detection utilizing Cas13d (CasRx). The technical details of most technologies is summarized in Table S1.

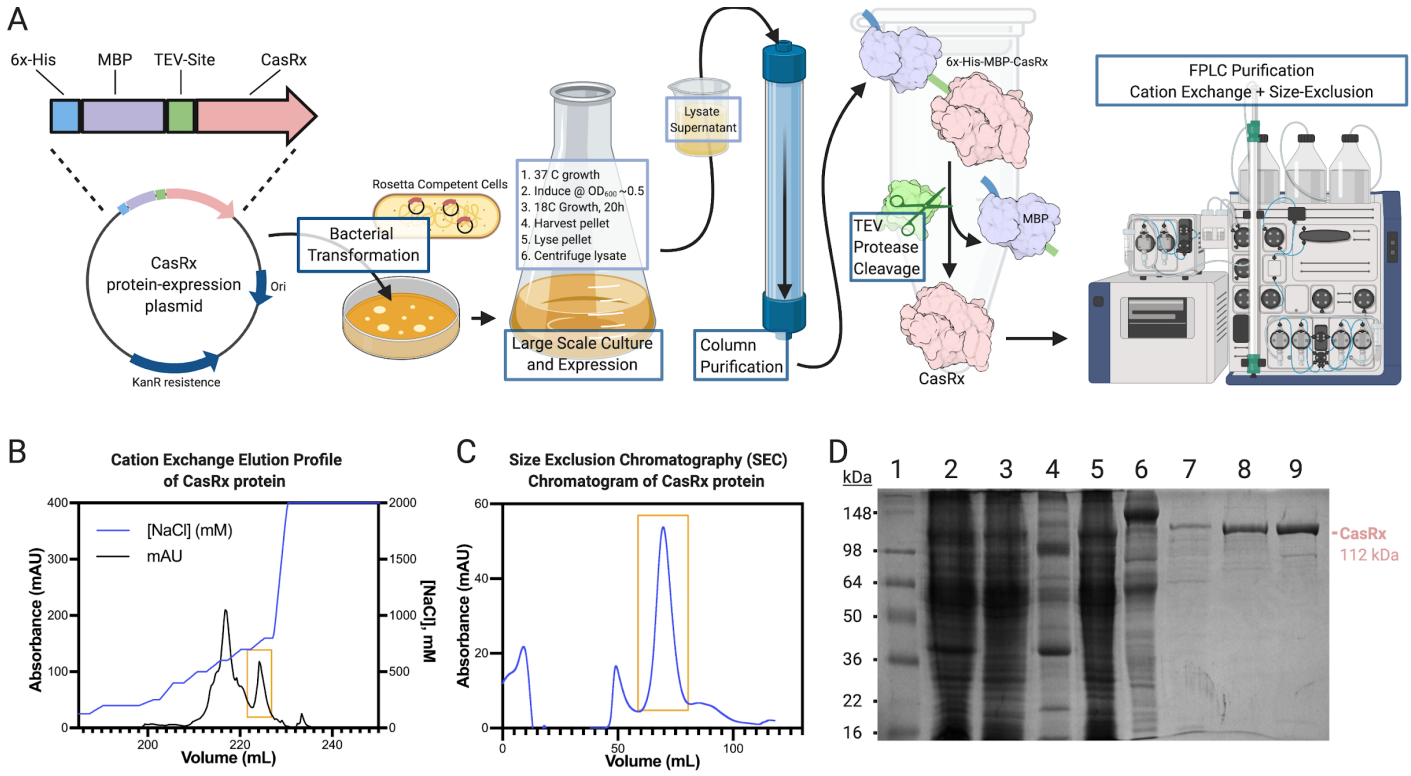


**Supplementary Figure 2. CasRx protein purification workflow and quality control. [A]** CasRx protein was produced and purified essentially as described in (Konermann et al. 2018). A CasRx protein-expression plasmid was generated with CasRx (pink) downstream of a Maltose-binding protein (MBP, purple) domain with an N-terminal 6xHis tag (blue), connected by a TEV protease cleavage sequence (green). Origin of replication and KanR cassette shown in navy. Transformation of the plasmid into Rosetta2 (DE3) Competent *E. coli* was followed by large scale culture growth. Cell lysate supernatant containing 6xHis-MBP-CasRx soluble hybrid protein was run on a Ni-NTA column for purification by affinity chromatography. CasRx protein was then released from the 6xHis-MBP moiety by TEV protease cleavage during O/N dialysis, and was further purified by cation exchange and size exclusion using Fast Protein Liquid Chromatography (FPLC). **[B]** The cation exchange elution profile of CasRx with the concentration of NaCl (mM) shown in blue. Peak containing CasRx recombinant protein (boxed in gold) elutes at ~700 mM NaCl. **[C]** The SEC elution profile of CasRx recombinant protein following Size Exclusion Chromatography (SEC) (blue). Peak containing CasRx recombinant protein highlighted boxed in gold. **[D]** A 10% SDS-PAGE gel showing protein species present at different stages of the purification protocol. Lane 1 is SeeBlue Plus2 Pre-stained Protein Standard with the predicted final CasRx protein size marked at right in pink at approximately 112 kDa. Lane 2 is a resuspended cell pellet. Lane 3 is cell lysate supernatant. Lane 4 is cell lysate pellet. Lane 5 is Ni-NTA flow through. Lane 6 is Ni-NTA Elution. Lane 7 is the sample post O/N Dialysis. Lane 8 is the sample after IEC, and Lane 9 is the concentrated Final Sample post-SEC.

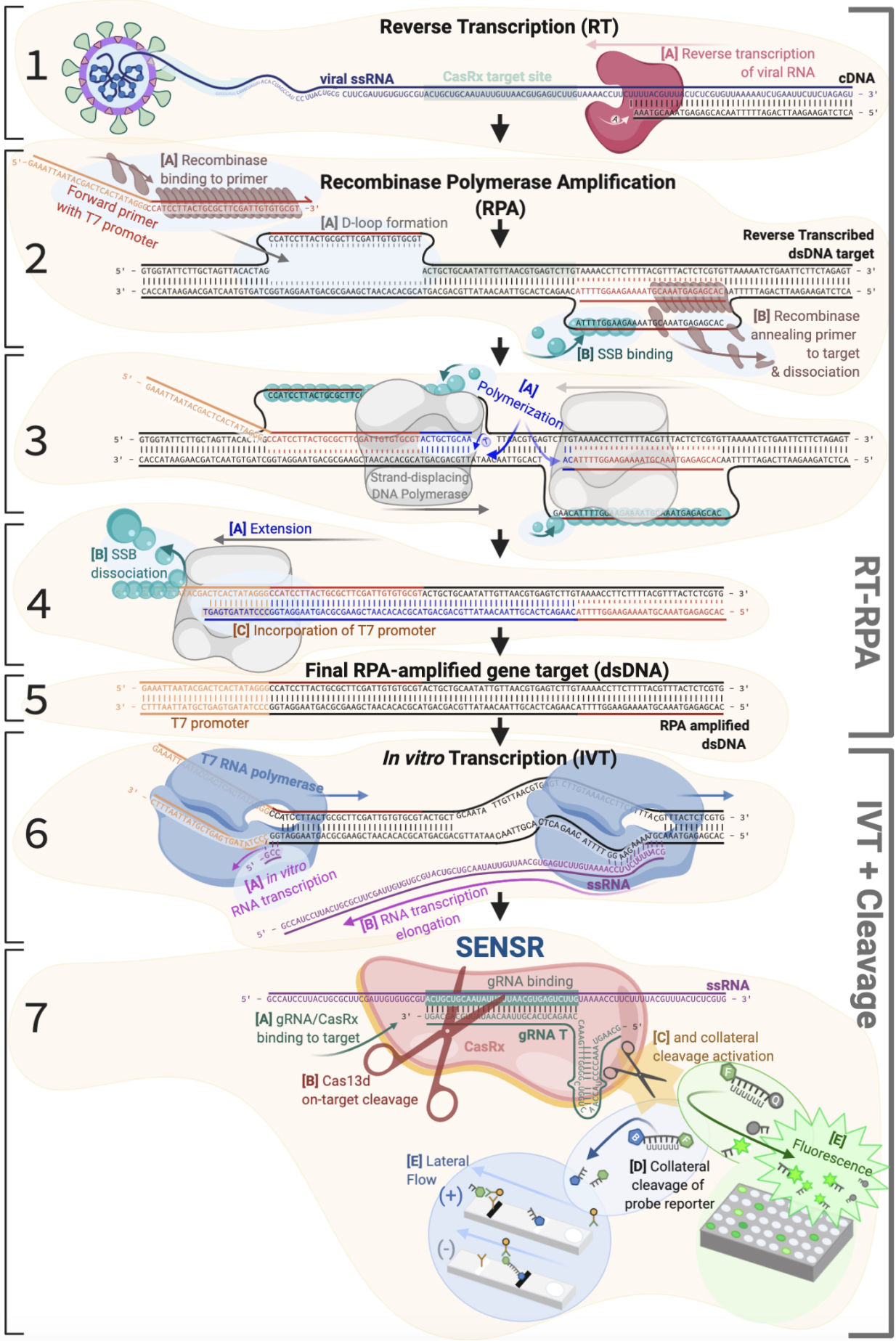
RT-RPA
IVT + Cleavage
1
Reverse Transcription (RT)
viral ssRNA
CasRx target site
[A] Reverse transcription of viral RNA
cDNA
2
[A] Recombinase binding to primer
Forward primer with T7 promoter
Recombinase Polymerase Amplification (RPA)
[A] D-loop formation
Reverse Transcribed dsDNA target
[B] SSB binding
[B] Recombinase annealing primer to target & dissociation
3
[A] Polymerization
Strand-displacing DNA Polymerase
4
[A] Extension
[B] SSB dissociation
[C] Incorporation of T7 promoter
5
Final RPA-amplified gene target (dsDNA)
T7 promoter
RPA amplified dsDNA
6
In vitro Transcription (IVT)
T7 RNA polymerase
[A] in vitro RNA transcription
[B] RNA transcription elongation
ssRNA
7
SENSR
gRNA binding
ssRNA
[A] gRNA/CasRx binding to target
CasRx
gRNA T
[B] Cas13d on-target cleavage
[C] and collateral cleavage activation
[D] Collateral cleavage of probe reporter
[E] Fluorescence
[E] Lateral Flow
(+)
(-)

**Supplementary Figure 3. Molecular scale overview of CasRx detection protocol workflow.** Bracketed into the two base component reactions, RT-RPA or CCR. [**Panel 1A**] Viral ssRNA is extracted and reverse transcribed into cDNA. A fragment of the viral RNA (navy), with a CasRx target site highlighted (mint). Reverse transcriptase (raspberry) actively reverse transcribes the viral template into cDNA. [**Panel 2A**] In the simultaneous RPA reaction, recombinase (brown) binds to the primer (red and orange) with D-loops formed at binding sites. [**2B**] Recombinase helps anneal the primer to the target site, and single strand binding protein (SSB, teal) begins annealing to ssDNA to stabilize the strand. [**Panel 3A**] Strand-displacing DNA polymerase (grey) amplifies the target DNA, with continued binding of SSB to ssDNA for stabilization. [**Panel 4A**] DNA amplicon extension is completed, [**4B**] while polymerase simultaneously dislodges SSB, and [**4C**] the T7 promoter region (orange) is added to the amplicon via primer extension. [**Panel 5**] The final product of the RT-RPA reaction is a small amplified fragment of target DNA encompassing the CasRx target site, with a T7 promoter added for subsequent IVT. [**Panel 6A**] T7 RNA polymerase-based *in vitro* transcription (blue) occurs, initiated from the T7 promoter (orange) in order to generate ssRNA (magenta) required as the activation substrate of CasRx. [**6B**] Elongation of the ssRNA template takes place. **[Panel 7**] CasRx detection of on-target sequence, activation of collateral cleavage activity, and detection. [**7A**] The CasRx/gRNA complex (pink and green) recognize, [**7B**] bind to, and cleave (red scissors) the ssRNA viral target template (magenta). [**7C**] This action activates the collateral cleavage property of CasRx (gold, black scissors). [**7D**] Following activation, collateral cleavage of an included small ssRNA probe can be analyzed via [**7E**] fluorescence or lateral flow assay.

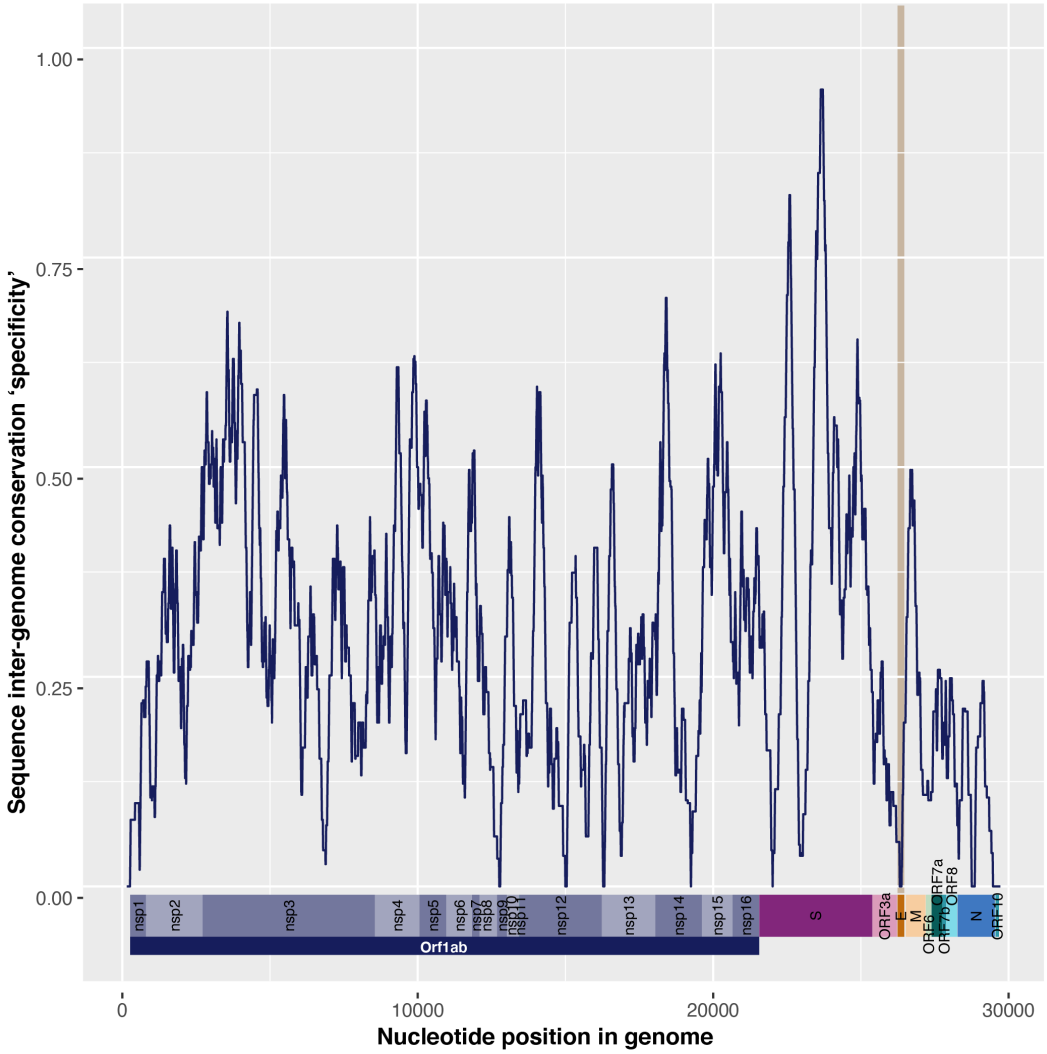


**Supplementary Figure 4. Depiction of unique gRNA target sequences across SAR-CoV-2 genome.** Spread of unique and specific 30 nt putative gRNA target sequences (Table S3-S5) displayed across the SARS-CoV-2 genome, smoothened over a 301 nt window. Higher specificity score indicates higher density of unique and conserved targets. Representative genome map shown at bottom with ORFs and genes annotated. E-gene ORF highlighted in orange with beige vertical bar highlighting the zero specificity score of the gene.

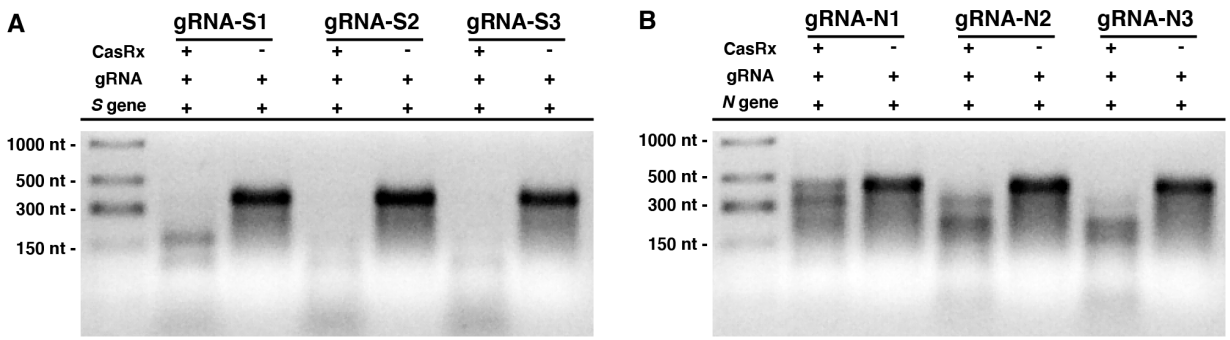


**Supplementary Figure 5. Preliminary assessment of candidate guides assayed in this study. [A]** Characterization of *Spike* gene gRNA cleavage activity for the three selected candidate guides. Each gRNA was incubated with the S-gene target template (350 nt) in the presence or absence of CasRx for 60 minutes. Cleavage reactions were run on 2% agarose 1xTBE gel for 30 minutes to resolve products. **[B]** Characterization of *Nucleocapsid* gene gRNA cleavage activity for the three selected candidate guides. Each gRNA was incubated with the N-gene target template (407 nt) in the presence or absence of CasRx for 60 minutes. Cleavage reactions were run on 2% agarose 1xTBE gel for 30 minutes to resolve products.

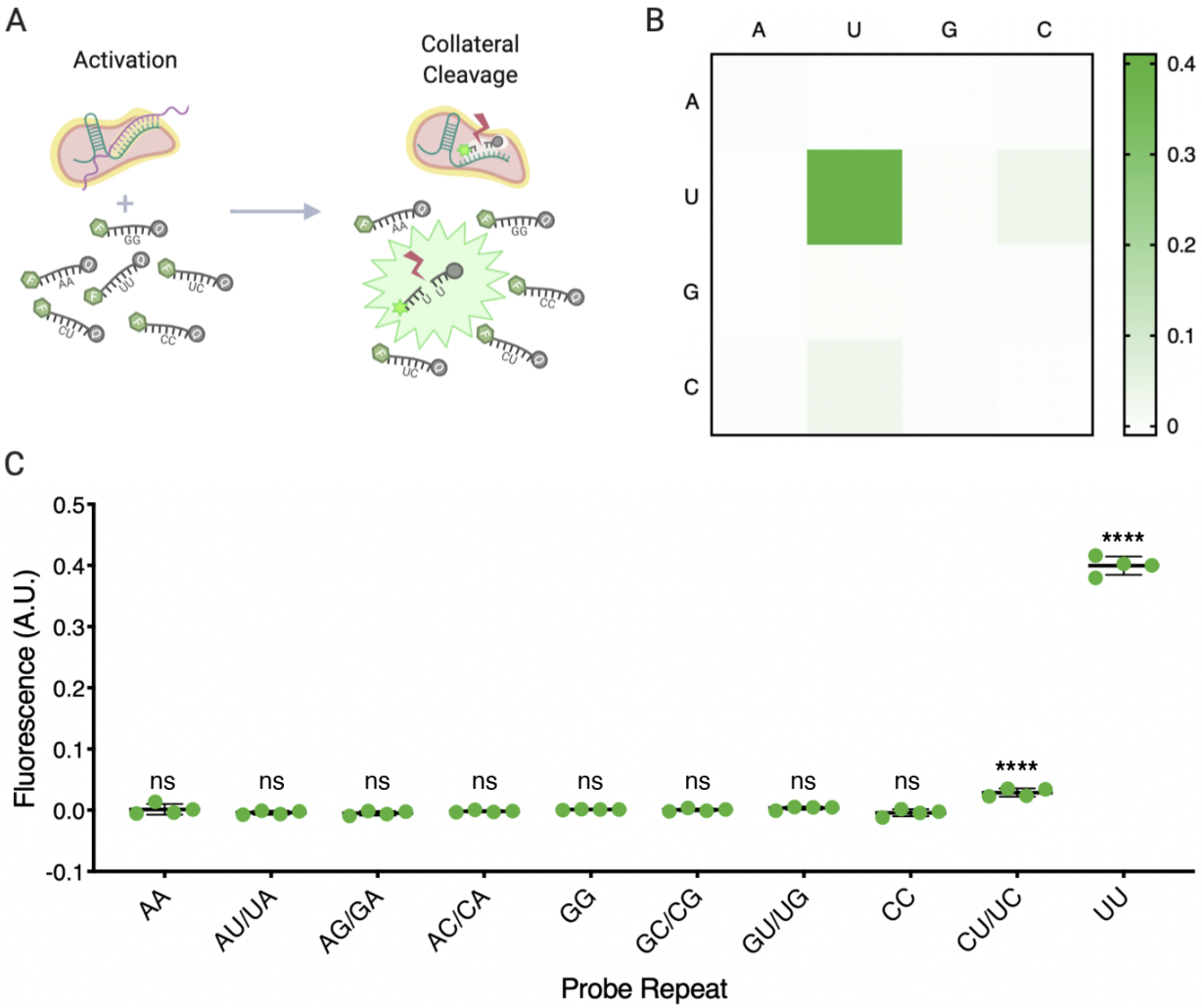


**Supplementary Figure 6. Probe di-nucleotide preference selection for SENSR fluorescence detection assay.** **[A]** Schematic representation of experiment determining the collateral cleavage, di-nucleotide preference for CasRx. **[B]** Heat map layout of background subtracted fluorescence normalized to NTC controls from CasRx collateral cleavage for all di-nucleotide probe combinations. The more saturated the color, the larger the increase in fluorescence. **[C]** Scatter plot of background subtracted fluorescence of experimental group normalized to NTC controls for all di-nucleotide probes calculated after 60 minutes of acquisition. A.U., Arbitrary Units. Data represents mean ± s.d. from quadruplicate measurements. Significance is representative of Šídák's multiple comparisons test.

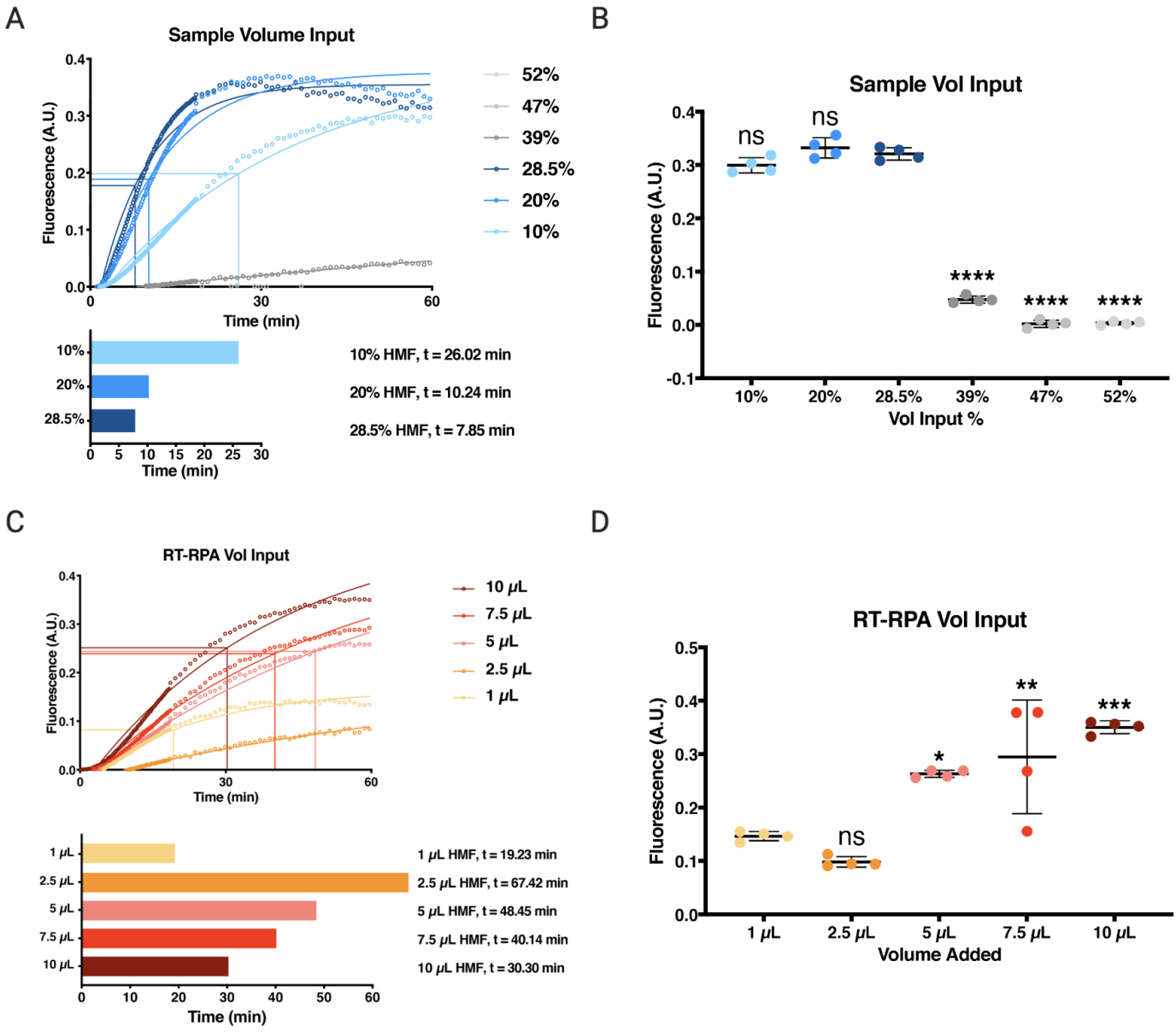


**Supplementary Figure 7. Optimization of SENSR volume input parameters. [A]** Assessment of sample volume input into RT-RPA reaction by volume percentage. RT-RPA reactions were run for 45 minutes with gRNA-N1 primers targeting 1000 copy/µL of synthetic *Nucleocapsid* template. Data were acquired for 60 minutes and then plotted to perform HMF analysis. 39%, 47%, and 52% v/v sample input HMF not shown in plot: 39% = 238.76 min, 47% = N/A, 52% = N/A. Intersecting lines represent the location of HMF for each group. **[B]** Scatter plot of background subtracted fluorescence data normalized to NTCs after 60 minutes of acquisition. A.U., Arbitrary Units. Data represents mean ± s.d. from quadruplicate measurements. Significance is representative of Dunnett's multiple comparisons test comparing all groups to 28.5% sample volume input group. **[C]** Assessment of RT-RPA volume added to CCR. Analysis was performed on 1000 copy/µL of synthetic *Nucleocapsid* template with gRNA-N3, which exhibited the second slowest HMF time in the preliminary gRNA analysis. Data were acquired for 60 minutes and then plotted to perform HMF analysis. Intersecting lines represent the location of HMF for each group. **[D]** Scatter plot of background subtracted fluorescence data normalized to NTCs after 60

minutes of acquisition. A.U., Arbitrary Units. Data represents mean ± s.d. from quadruplicate measurements. Significance is representative of Dunnett's multiple comparisons test comparing all groups to 1 μL RT-RPA volume input group.

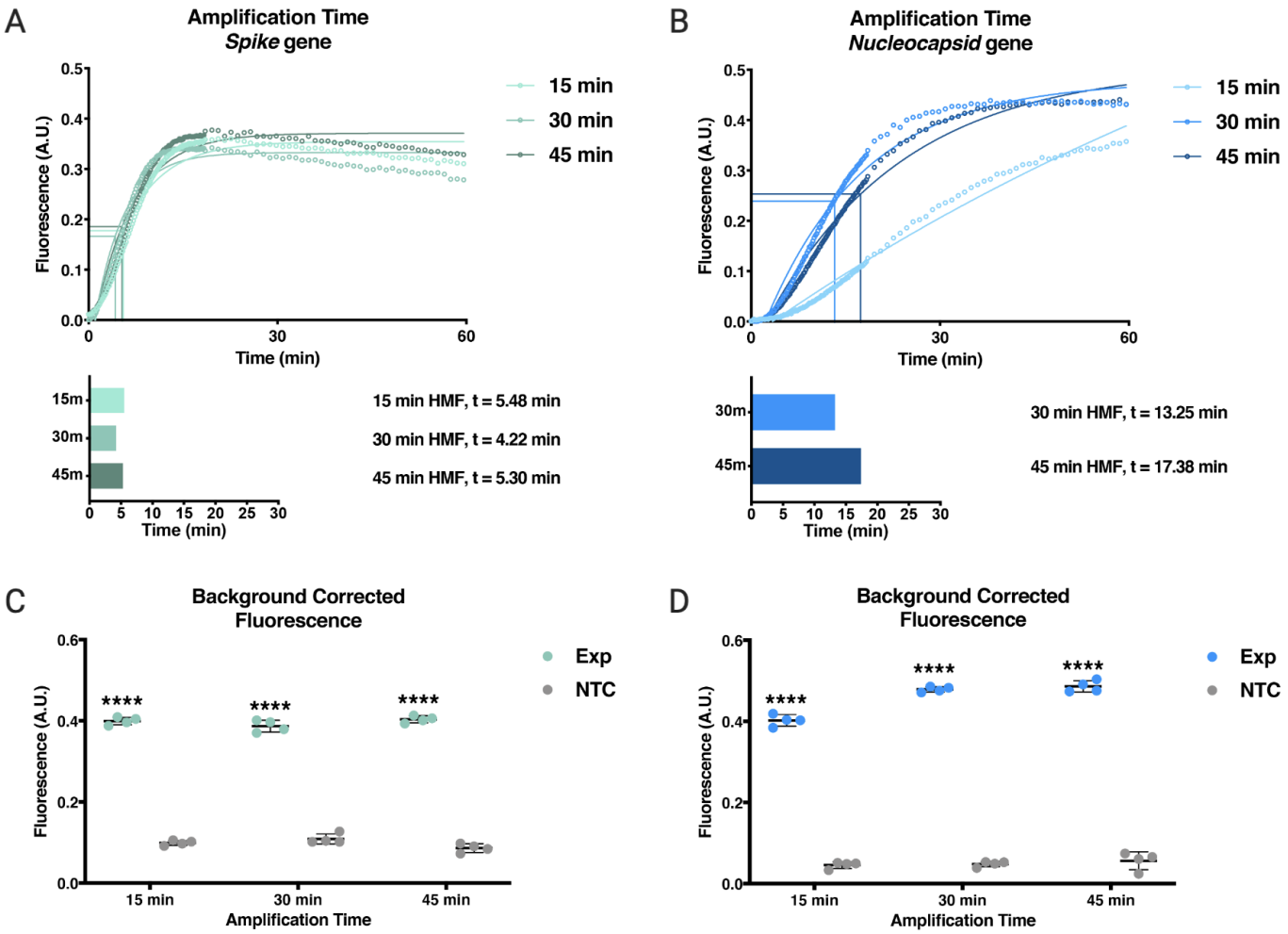


**Supplementary Figure 8. Assessment of optimal amplification time for detection of *Spike* and *Nucleocapsid* targets. [A]** Fluorescence plot of experimentals targeting 100 copy/µL of synthetic *Spike* template with gRNA-S3 normalized to NTC. Data were acquired for 60 minutes and then plotted to perform HMF analysis. Intersecting lines represent the location of HMF for each group. **[B]** Fluorescence plot of experimentals targeting 100 copy/µL of synthetic *Spike* template with gRNA-N1 normalized to NTC. Data were acquired for 60 minutes and then plotted to perform HMF analysis. 15 minute amplification HMF not shown in plot: 15m = 89.24 min. Intersecting lines represent the location of HMF for each group. **[C]** Scatter dot plot of background subtracted fluorescence for *Spike* targeting with gRNA-S3. Fluorescence signal plotted represents the final data acquired at 60 minutes subtracted by the initial fluorescence signal recorded. A.U., Arbitrary Units. Data represents mean ± s.d. from quadruplicate measurements. Significance is representative of Tukey's multiple comparisons test for experimentals compared to respective NTCs. **[D]** Scatter dot plot of background subtracted fluorescence for *Nucleocapsid* targeting with gRNA-N1. Fluorescence signal plotted represents the final data acquired at 60 minutes subtracted by the initial fluorescence signal recorded. A.U., Arbitrary Units. Data represents mean ± s.d. from quadruplicate measurements. Significance is representative of Tukey's multiple comparisons test for experimentals compared to respective NTCs.

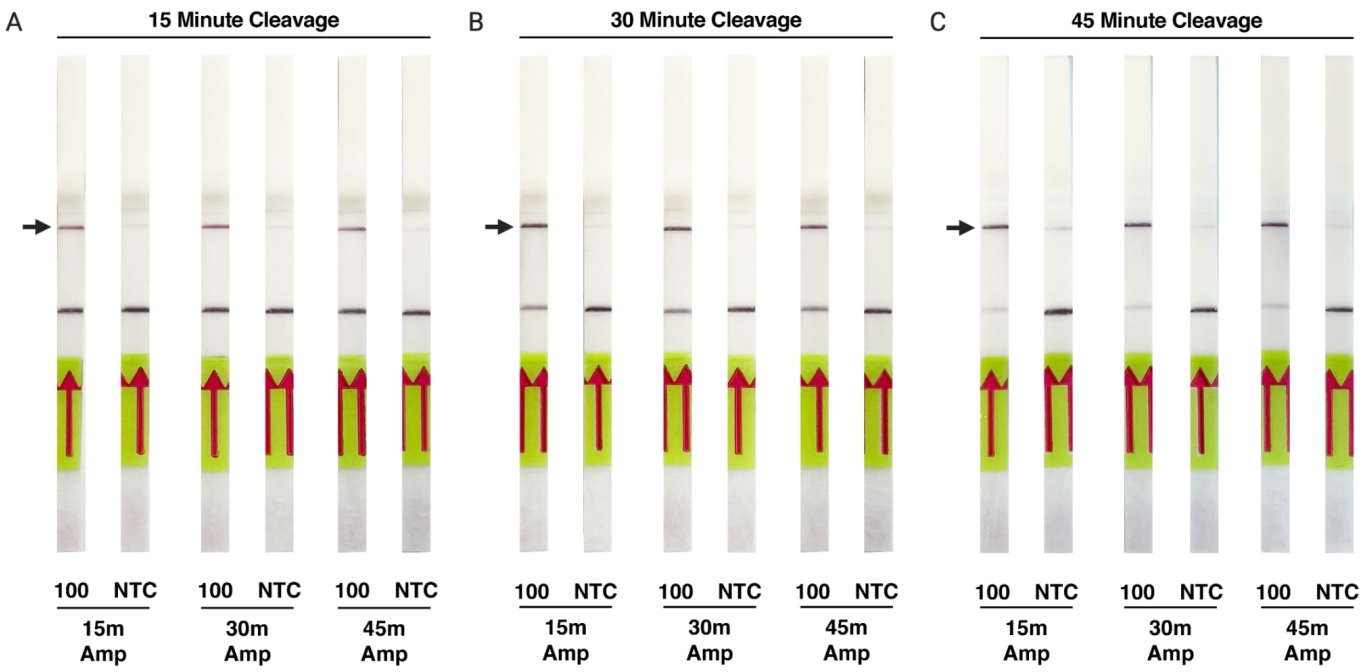


**Supplementary Figure 9. Optimization of amplification and cleavage time for lateral flow readout of SENSR. [A]** Lateral flow readout detecting SARS-CoV-2 *Spike* gene with gRNA-S3 after 15 minutes cleavage. The synthetic S gene was amplified via RT-RPA for 15, 30, or 45 minutes and then incubated in a CCR for 15 minutes. Lateral flow readout was then performed for 3 minutes. Detection determined increased saturation of test band (arrow). **[B]** Lateral flow readout after 30 minutes cleavage. **[C]** Lateral flow readout after 45 minutes cleavage.

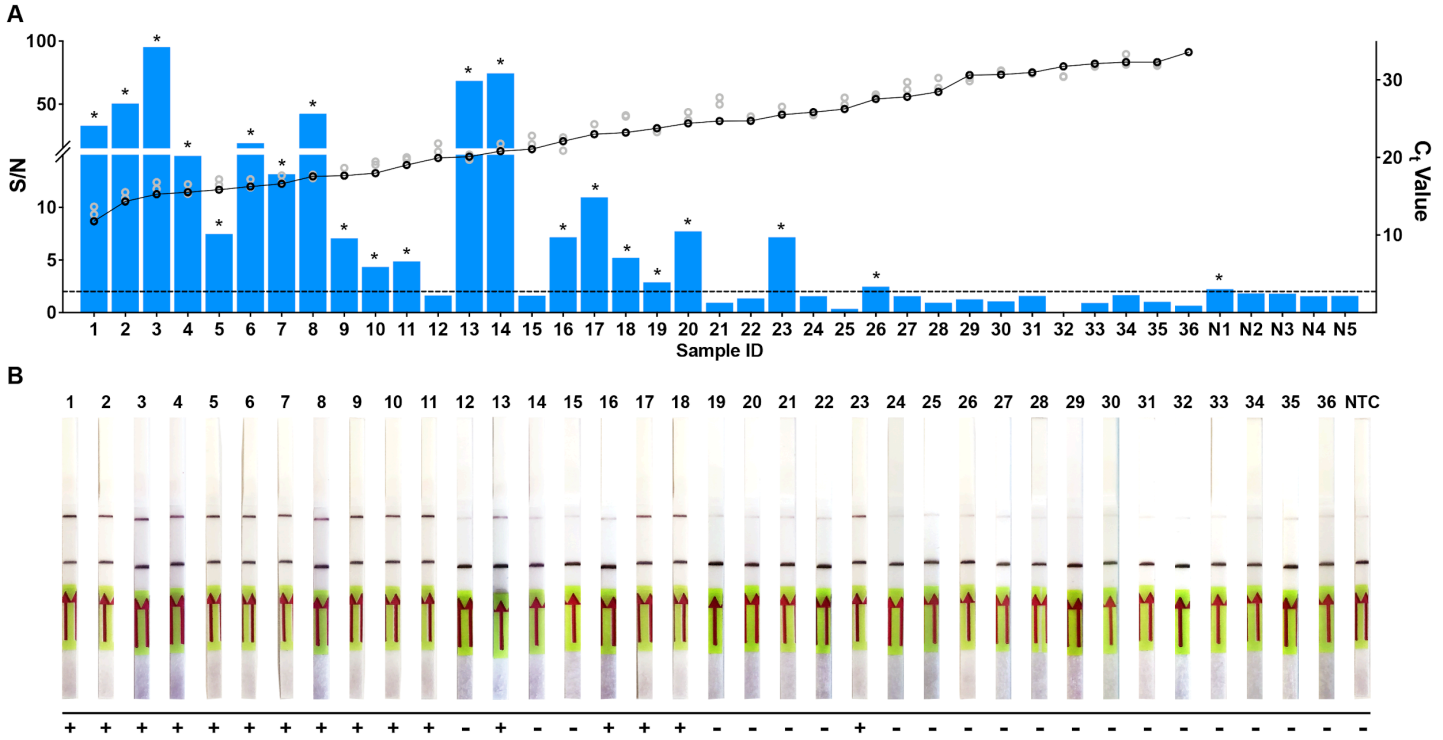


C

| | Positive Samples | | Negative Samples | |
|---|---|---|---|---|
| Fluorescence Analysis | 20/36 Positive | 23% False Negative Rate for $C_t \leq 27.5$ | 1/36 Positive | 2.8% False Positive Rate |
| Lateral Flow Analysis | 16/36 Positive | 38% False Negative Rate for $C_t \leq 27.5$ | 0/36 Positive | 0% False Positive Rate |

**Supplementary Figure 10. SENSR detection of positive SARS-CoV-2 validated patient samples with unoptimized protocol.** **[A]** SENSR fluorescence analysis of RT-qPCR validated patient samples using an N-targeting gRNA for detection. Signal-to-Noise (S/N) ratio of 36 positive and 5 negative samples are shown. Positive samples are listed in order from lowest to highest $C_t$ value. Open circles represent $C_t$ value of N- (black), S- (gray), and Orf1ab (gray). The five negative samples are negative samples with the highest S/N ratio. Dashed line represents the S/N threshold = 2. Asterisks represent a S/N > 2. **[B]** Lateral flow based detection of the 36 positive and NTC for comparison. The top band (arrow) represents the test band and the bottom the control band. An increase in saturation of the top band indicates a positive detection of SARS-CoV-2 in the sample. Result of detection indicated below each test strip. **[C]** Summary of fluorescence and lateral flow detection results for the RT-qPCR validated positive and negative patient samples.

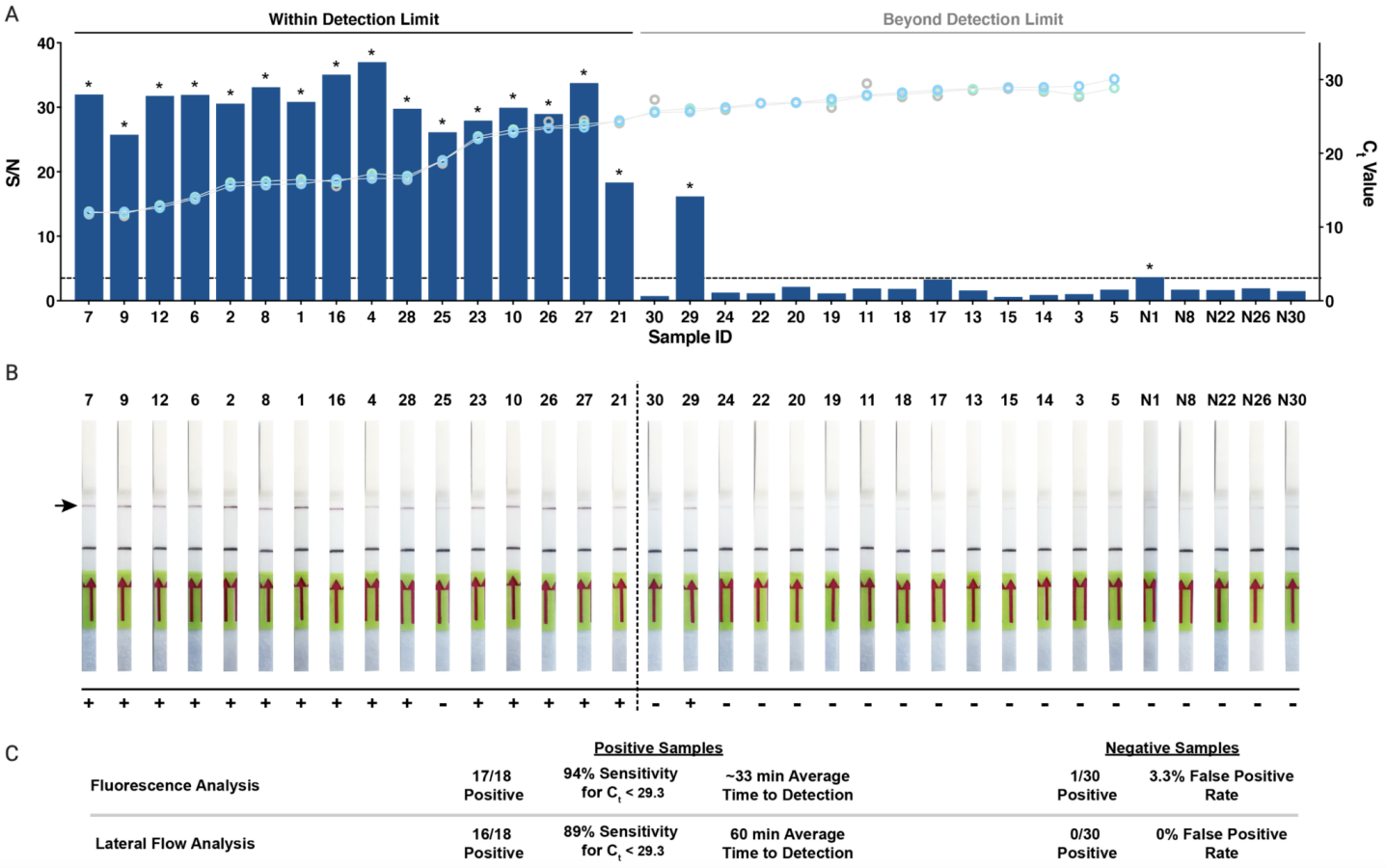


C

| | Positive Samples | | | Negative Samples | |
|---|---|---|---|---|---|
| Fluorescence Analysis | 17/18 Positive | 94% Sensitivity for $C_t$ < 29.3 | ~33 min Average Time to Detection | 1/30 Positive | 3.3% False Positive Rate |
| Lateral Flow Analysis | 16/18 Positive | 89% Sensitivity for $C_t$ < 29.3 | 60 min Average Time to Detection | 0/30 Positive | 0% False Positive Rate |

**Supplementary Figure 11. SENSR detection of positive SARS-CoV-2 validated patient samples. [A]** SENSR fluorescence analysis of RT-qPCR validated patient samples using gRNA-N1 for detection. Signal-to-Noise (S/N) ratio of 30 positive and 5 negative samples are shown. Positive samples are listed in order from lowest to highest $C_t$ value. Open circles represent $C_t$ value of S- (spindrift), N- (ice), and Orf1ab (gray). The five negative samples are negative samples with the highest S/N ratio. Dashed line represents the S/N threshold = 3.506. Asterisks represent a S/N > 3.506. **[B]** Lateral flow based detection of the 30 positive and 5 negative samples. The top band (arrow) represents the test band and the bottom the control band. An increase in saturation of the top band indicates a positive detection of SARS-CoV-2 in the sample. Result of detection indicated below each test strip. **[C]** Summary of fluorescence and lateral flow detection results for the RT-qPCR validated positive and negative patient samples.

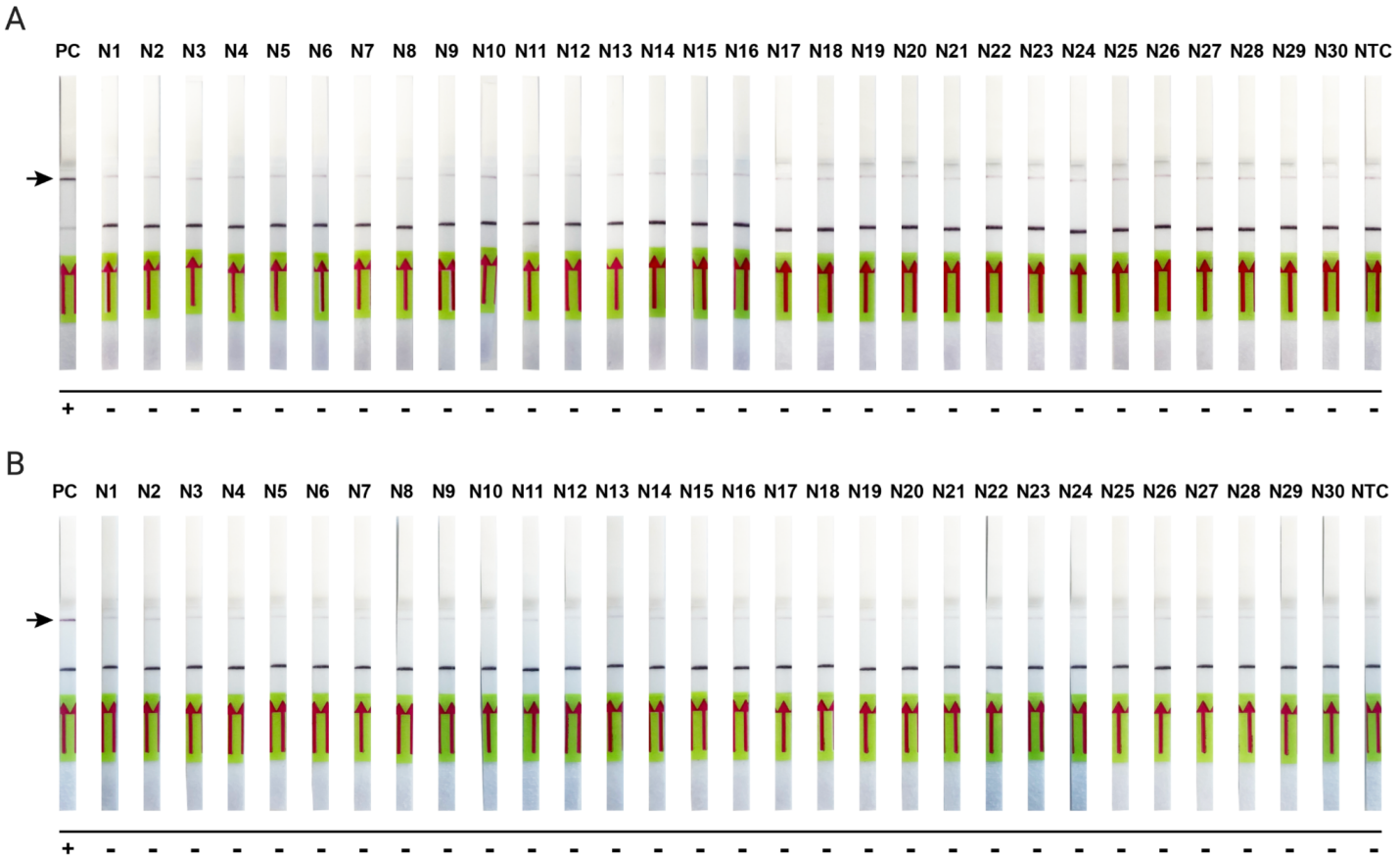


**Supplementary Figure 12. SENSR lateral flow analysis of RT-qPCR validated SARS-CoV-2 negative patient samples. [A]** SARS-CoV-2 negative patient samples challenged with gRNA-S3 (*Spike*) in LF detection assay (30 minutes RT-RPA/ 30 minutes CCR). Positive Control (PC) and No-Template Controls (NTC) were run in parallel. Positive result determined by increase in saturation in top band (arrow). **[B]** SARS-CoV-2 negative patient samples challenged with gRNA-N1 (*Nucleocapsid*) in LF detection assay (30 minutes RT-RPA/ 30 minutes CCR). Positive result determined by increase in saturation in top band (arrow).

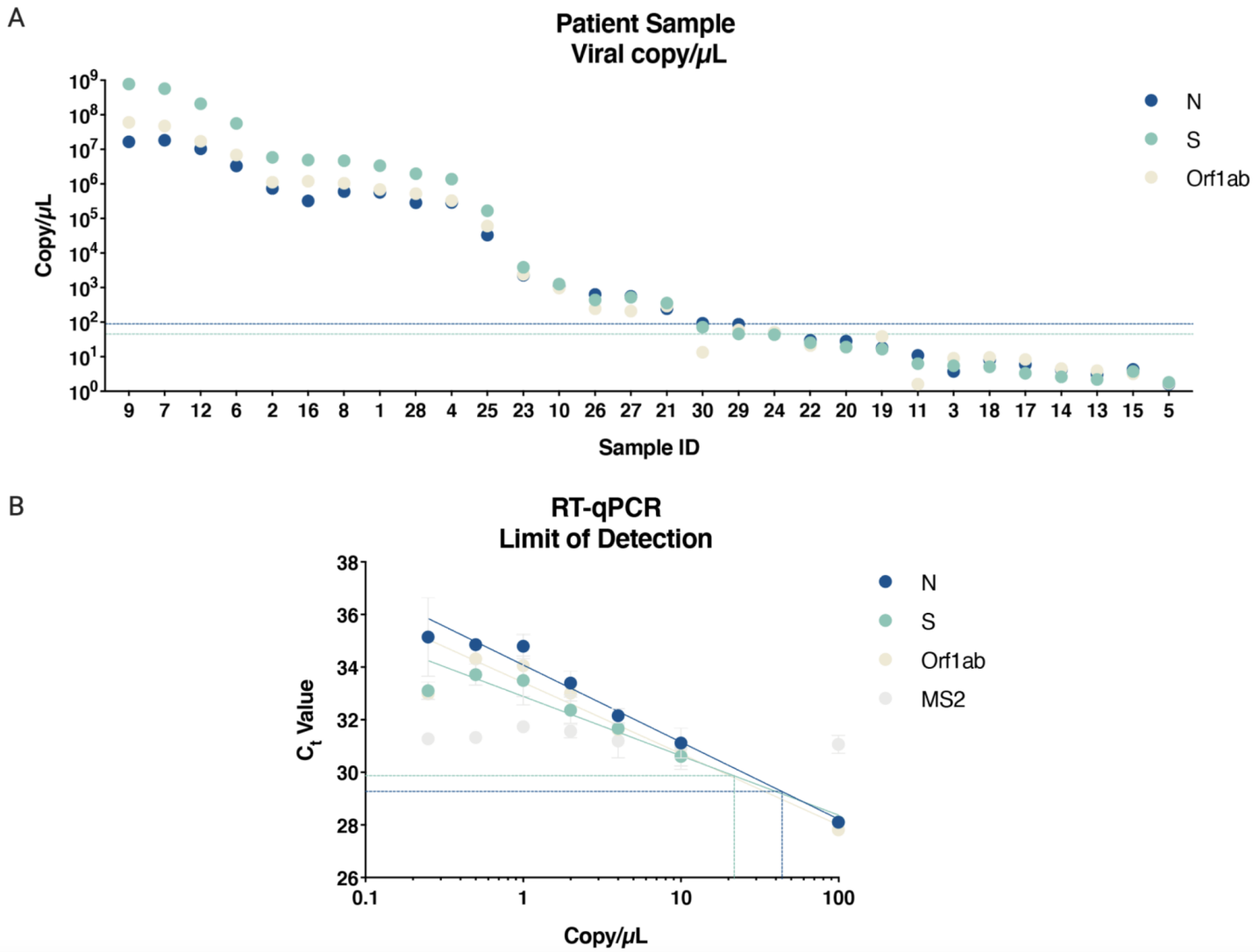


**Supplementary Figure 13. Viral copy number per µL for RT-qPCR verified positive samples. [A]** Conversion of $C_t$ value to copy/µL using nonlinear regression obtained from **[B]** for each positive patient sample analyzed. Horizontal dashed lines represent the detection limit for SENSR corrected for 2 µL input: S-gene (green; 45 copy/µL) and N-gene (blue; 89 copy/µL). **[B]** RT-qPCR LoD experiment for the three targets analyzed via RT-qPCR (N- blue, S-green, and Orf1ab-beige). Semi-log nonlinear regression analysis was performed to generate a line of best fit. RT-qPCR analysis was performed with 2 µL of sample input. Intersecting lines represent the copy/µL and $C_t$ value detection limit for SENSR analysis of S-gene (green; $C_t$ = 29.87, copy/µL = 21.78) and N-gene (blue; $C_t$ = 29.27, copy/µL = 43.76).

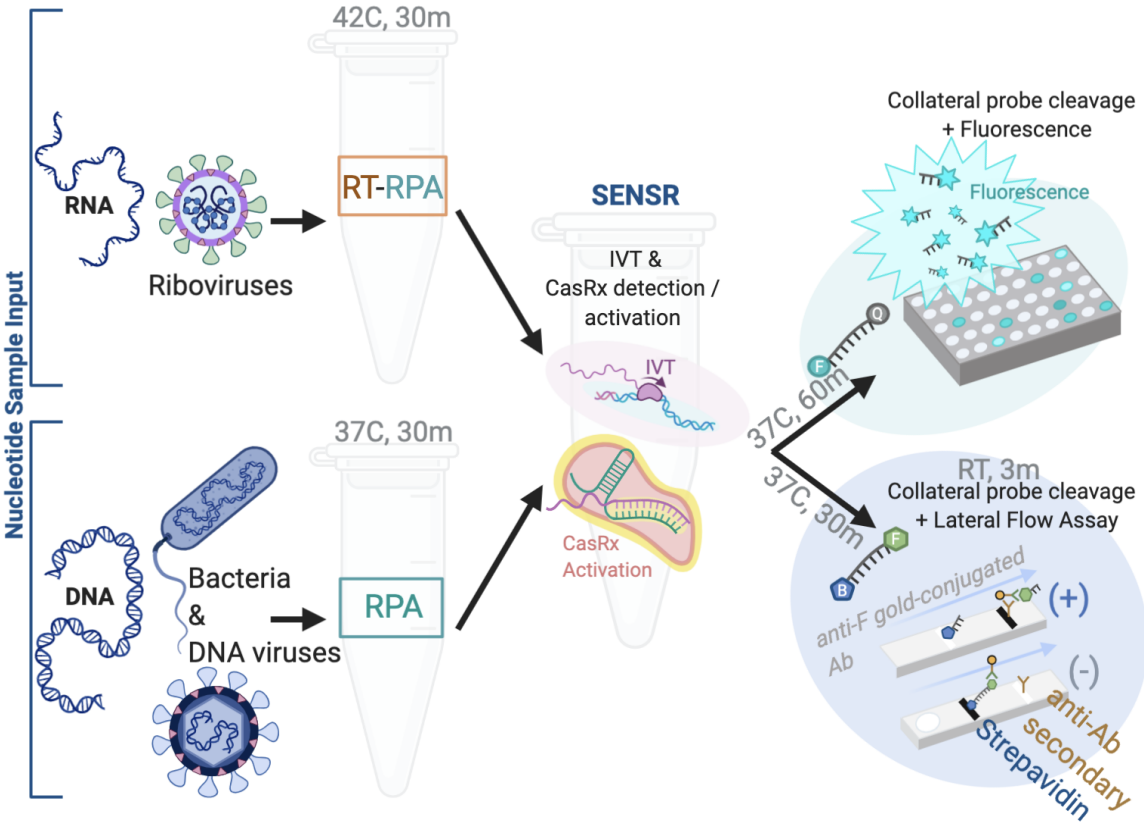


**Supplementary Figure 14. Schematic representation of SENSR application for detection of other pathogens.** In addition to RNA-based templates (top row), SENSR technology could also be used for DNA-based templates, including, but not limited to, bacterial samples (shown) as well as DNA viruses such as herpes (shown, bottom, navy). DNA-based sample templates can be input directly into the RPA amplification reaction, negating the need for a simultaneous reverse transcription (RT) reaction as is required for RNA-based templates. Like SENSR on RNA-based templates, the reaction occurs in two steps. The first amplification step, RT-RPA or RPA, is followed by the SENSR reaction which is identical regardless of initial input molecular species. This reaction is composed of simultaneous *in vitro* transcription (IVT) as well as CasRx cleavage and activation of collateral cleavage activity. The assay can be read out by fluorescence or lateral flow in the same fashion regardless of DNA or RNA sample input.

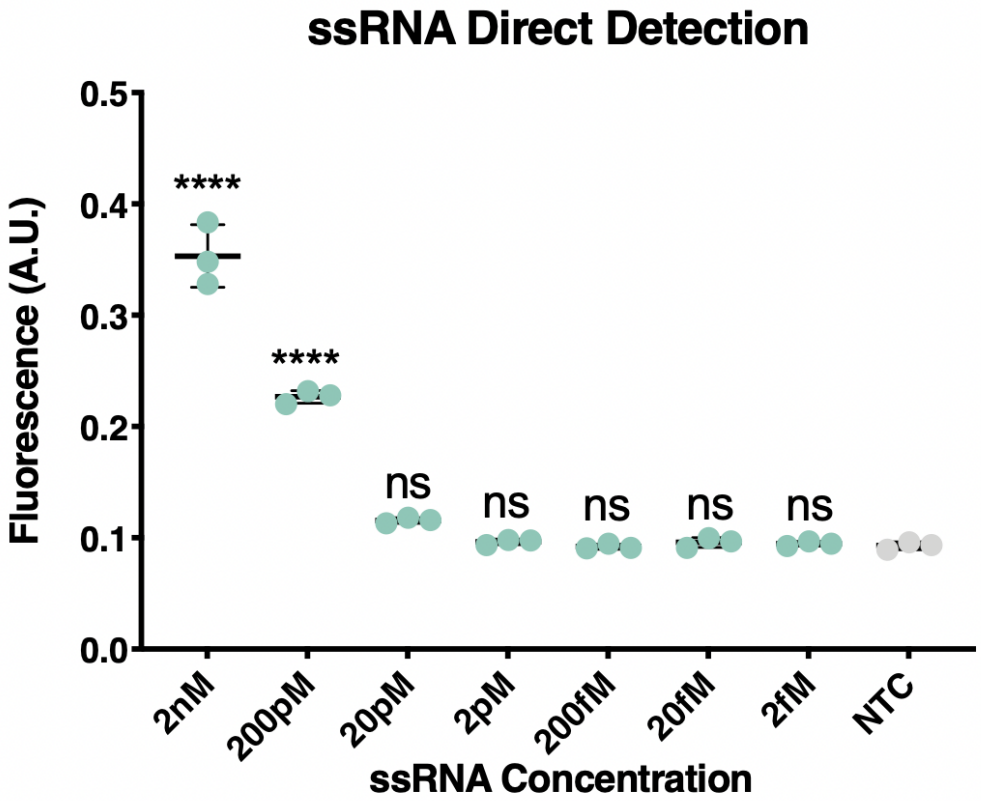


**Supplementary Figure 15. CasRx direct detection of synthetic Spike ssRNA.** Varied concentrations of synthetic ssRNA Spike template incubated directly with CasRx and gRNA-S3 without preamplification. Fluorescence signal plotted represents the final data acquired at 30min subtracted by the initial fluorescence signal recorded. A.U., Arbitrary Units. Data represents mean ± s.d. from triplicate measurements. Significance is representative of Dunnett's multiple comparisons test for experimentals compared to NTC.

**----------SUPPLEMENTARY TABLES----------**

## Supplementary Tables

**Table S1.** Summary Table of current CRISPR-based anti-Covid technologies.

**Table S2.** Analysis identifying putative 30 nt CasRx gRNA target sites conserved across, and specific to, the SARS-CoV-2 genome.

**Table S3.** Predicted unique and conserved 30 nt CasRx gRNA target sequences to SARS-CoV-2.

**Table S4.** List and sequences of reagents generated and used throughout this work. Primers for cloning, gRNA prep, and RT-RPA, as well as gRNA sequences, viral gene templates, plasmid sequences and probes.

**Table S5.** RT-RPA protocols for sample volume input variation experiments.

**Table S6.** CCR protocols for RT-RPA volume variation experiments.

**Table S7.** Data from RT-qPCR and SENSR fluorescence analysis of patient samples for detection of SARS-CoV-2.

**Table S8.** Time-to-detection from fluorescence analysis of all positive patient samples**.**

**----------SUPPLEMENTARY VIDEO----------**

## Supplementary Video

**Supplementary Video 1.** Video of gRNA-S3 LoD experiment. Video representation of lateral flow readout performed against S-gene synthetic RNA template diluted to concentrations on a logarithmic scale from 10,000 to 10 copy/µL. Lateral flow strips were incubated for 3 min. The video is sped up by 7.5x. Tubes (from left to right): 10,000 copy/µL, 1,000 copy/µL, 100 copy/µL, 10 copy/µL, and NTC.

**----------SUPPORTING INFORMATION----------**

**CasRx subcloning, protein expression and purification**

To produce an expression plasmid for CasRx protein production, we cloned the human codon optimized CasRx coding sequence into the expression vector, pET-His6-MBP-TEV-yORF (Series 1-M) (purchased from QB3 MacroLab, Berkeley) using the Gibson assembly method (Gibson et al., 2009). In brief, the CasRx coding sequence was PCR amplified from plasmid OA-1050E (Addgene plasmid # 132416 [31]) using primers 1136I.C1 and 1136I.C2 (**Table S4**). The fragment was purified and subcloned into the restriction enzyme cutting site EcoRI, downstream of the His-MBP recombinant protein in pET-His6-MBP-TEV-yORF, generating the final pET-6xHis-MBP-TEV-CasRx (OA-1136J; Addgene plasmid # 153023) plasmid.

Protein expression, culture, cell lysis, affinity and further downstream protein purification were performed as previously described (**Fig S2**)[30]. In brief, to facilitate protein expression, pET-His6-MBP-TEV-CasRx was transformed into Rosetta2 (DE3) pLysS cells (Novagen, 71403). Starter cultures in LB were incubated at 37°C O/N. 20 mL of starter culture were used to inoculate 1L of TB media supplemented with antibiotics. Cultures were allowed to grow until $OD_{600}$ ~0.5, cooled on ice, induced with 0.2mM IPTG, and then grown for 20 hrs at 18°C. Cells were then pelleted, freeze-thawed, resuspended, lysed by sonication and clarified by centrifugation. Protein purification was performed by gravity Ni-NTA affinity chromatography (Thermo Scientific HisPur Ni-NTA Resin) followed by removal of the 6xHis-MBP tag by TEV protease concurrently with O/N dialysis. Further purification was achieved by cation exchange using a 5-mL HiTrap SP HP using a gradient of 125mM to 2M NaCl in 50mM Tris-HCl, 7.5% v/v glycerol, 1mM DTT. The protein was finally purified by gel filtration chromatography in 50mM Tris-HCl, 600mM NaCl, 10% glycerol, 2mM DTT on a Superdex 200 16/600 column. Fractions were pooled, concentrated to ~2mg/mL and stored at -80ºC in the same buffer.

**Bioinformatics of SARS-CoV-2 SENSR target sites**

433 SARS-CoV-2 genomes were downloaded from NCBI Virus (https://www.ncbi.nlm.nih.gov/labs/virus/vssi/#/virus?SeqType_s=Nucleotide&VirusLineage_ss=SARS-CoV-2,%20taxid:2697049) and 3,164 non-SARS-CoV-2 Coronavirinae genomes were downloaded from Virus Pathogen Resource (https://www.viprbrc.org/brc/home.spg?decorator=corona_ncov) on April 7, 2020. All possible 30nt sequences were extracted from the two genome sets using a Perl script (**File S1**) generating 52,712 and 8,338,305 unique fragments from SARS-CoV-2 and non-SARS-CoV-2 genomes, respectively. 16,645 30nt sequences that perfectly matched all 433 SARS-CoV-2 genomes were filtered to remove the ones that were also found in any of the 3,164 non-SARS-CoV-2 genomes to produce a set of 8,846 SARS-CoV-2-specific sequences (**Table S4**). The guides were then mapped to the human transcriptome (GRCh38, ENSEMBL release 99, ftp://ftp.ensembl.org/pub/release-99/fasta/homo_sapiens/) comprising both coding and non-coding RNAs using bowtie 1.2.3 allowing up to two mismatches (-v2). gRNA density was calculated using a sliding window of 301nt for each position of the reference SARS-CoV-2 genome NC_045512 (https://www.ncbi.nlm.nih.gov/nuccore/NC_045512) and plotted in R (**Fig S3**). Viral genes that are affected by each gRNA were identified using the intersect function of bedtools (**Table S3**).

**Production of target SARS-CoV-2 RNA and gRNAs**

Two synthetic dsDNA gene fragments containing an upstream T7 promoter sequence corresponding to the SARS-CoV-2 *Spike* (S) and *Nucleocapsid* (N) protein coding regions were generated (GeneBank Accession # MN908947). The 375bp SARS-CoV-2 S-gene segment was ordered and synthesized as a custom gBlock from Integrated DNA Technologies (IDT) and amplified using primers 1136AE-F and 1136AE-R (**Table S4**). A 431bp SARS-CoV2 N-gene segment was amplified from a plasmid 1136Y (Catalog # 10006625) [39] using primers

1136X2-F and 1136X2-R (**Table S4**). These two SARS-CoV-2 gene targets were amplified using PCR and then purified using the MinElute PCR Purification Kit (QIAGEN #28004).

We designed gRNAs targeting the SARS-CoV-2 gene segments using criteria previously outlined (**Fig 1B**) [31] and generated these following a previously described templateless PCR protocol [43]. The primers used to amplify these gRNAs, as well as their final sequence are outlined in **Table S4**. We synthesized both the synthetic SARS-CoV-2 templates and gRNAs through *in vitro* transcription (IVT) using MEGAscript T7 Transcription Kit (Invitrogen #AM1334), followed by DNaseI digestion and purification using the MEGAclear Transcription Clean-Up Kit (Invitrogen #AM1908).

**Half-Maximum Fluorescence analysis**

Half-maximum fluorescence (HMF) analysis was used to determine which gRNA cleaved the modified ssRNA probe fastest. The HMF time-point was calculated by fitting a non-linear regression ( $y = Y_M - (Y_M - Y_0)^{(-k*x)}$, where $Y_M$ = maximum fluorescence, $Y_0$ = initial fluorescence, $k$ = rate constant, and $x$ = time) to the averaged and normalized fluorescence over time data for each gRNA. The equation for the non-linear regression was then used to solve for $x$, or time (min) ($x = ((ln(Y_M - y) - ln(Y_M - Y_0))/(-k)$ ), by entering in HMF fluorescence value recorded for $y$.

**Patient samples ethics statement**

Human samples from patients were collected under University of California San Diego's Human Research Protection Program protocol number 200470 for negatives (PI: Lauge Farnaes), and under a waiver of consent from clinical samples from San Diego County for positives (PI: Kristian Andersen), as part of the SEARCH Alliance activities. Samples were de-identified as required by these protocols prior to testing and analysis under University of California San Diego Biological Use Authorization protocols R1806 and 2401.

**RNA extraction and processing of patient samples**

Patient nasopharyngeal (NP) samples were collected and RNA was extracted using Omega Bio-Tek Mag-Bind Viral DNA/RNA 96 Kit (Omega Cat. No. M6246-03), following the manufacturer's protocol for the KingFisher Flex platform.

**RT-qPCR validation of SARS-CoV-2 infection in patient samples**

Patient samples were determined to be SARS-CoV-2 positive or negative using TaqPath COVID-19 Combo Kit RT-qPCR assay as described in (https://www.fda.gov/media/136112/download), and reducing the RT-qPCR reaction volumes to 3µL and diluting the MS2 phage control to improve the LoD of the assay. The presence of SARS-CoV-2 vRNA was analyzed using primers targeting the N, S, and Orf1ab genes with an MS2 control. All RT-qPCR assays were run using TaqPath 1-Step RT-qPCR Master Mix (ThermoFisher #A15299) and thermocycling conditions were run following the CDC recommended protocol (https://www.fda.gov/media/136112/download). Fluorescence data were acquired on a QuantStudio 5 qPCR machine (Applied Biosystems).